

Biosynthesis of Prion Protein Nucleocytoplasmic Isoforms by Alternative Initiation of Translation*

Received for publication, May 28, 2008, and in revised form, December 5, 2008 Published, JBC Papers in Press, December 5, 2008, DOI 10.1074/jbc.M804051200

María E. Juanes[‡], Gema Elvira[‡], Aranzazu García-Grande[§], Miguel Calero[¶], and María Gasset^{‡1}

From the [‡]Instituto de Química-Física "Rocasolano, Consejo Superior de Investigaciones Científicas (CSIC)," Serrano 119, 28006 Madrid, the [§]Centro Nacional de Investigaciones Oncológicas, Melchor Fernández Almagro 3, 28029 Madrid, and the [¶]Centro Nacional de Microbiología, Instituto de Salud Carlos III, Carretera Pozuelo Km 2, 28220 Majadahonda, Madrid, Spain

The cellular prion protein PrP^C is synthesized as a family of

Of these different members, CytPrP, accounts for a minor

WITHDRAWN
October 27, 2017

This article has been withdrawn by the authors. We have become aware of errors in the preparation of Figs. 2 and 3, where some lanes appear duplicated. Although replicated experiments performed at the time support the results and conclusions presented in the published paper, we believe that the responsible course of action is to withdraw the article in the interests of maintaining the publication standards of the journal. We apologize for any inconvenience we may have caused. The paper with the corrected figures can be obtained by contacting the authors.

neurodegenerative diseases through its conversion into self-perpetuating and neurotoxic forms (1–4). Despite a large amount of evidence supporting a role in survival/death and growth/differentiation cell decisions, the physiological function of PrP^C and its involvement in disease remain elusive (5–8). A crucial limiting factor for PrP^C functional determination is its molecular diversity. Although PrP^C is mainly thought of as a glycoprotein attached to the cell surface by a glycosylphosphatidylinositol anchor, PrP^C is actually synthesized as a family of four members: the membrane anchored glycoprotein (SecPrP), two transmembrane forms with opposite topologies (NtmPrP and CtmPrP), and a soluble form (CytPrP) (3, 9–12).

decipher this code and use it as a tool to isolate its synthesis from that of the major forms and inspect its function. We have found that CytPrP is indeed a novel PrP isoform that accesses the nucleus and interferes with cell growth. These results provide new insights on PrP diversity and its role in health and disease.

EXPERIMENTAL PROCEDURES

Plasmid Construction and Recombinant Standard Production—The plasmid pcDNA4-HaPrP, kindly provided by Dr. R. S. Hegde, was first mutated to introduce the six nucleotides from the 5'-untranslated region adjacent to the initial ATG to preserve the wild type Kozak sequence. The HuPrP open reading frame was cloned into pcDNA3.1 at BamHI/EcoRI sites preserving the corresponding wild type Kozak region. Wild type constructs were used as templates to generate different mutants (see Table 1 and Fig. 1) by using the Quikchange protocols (Stratagene). The integrity of each construct was verified by sequencing. Recombinant PrP chains of 1–254, 15–231, 15–254, and 23–231 were produced from the corresponding pET11a plasmids in *Escherichia coli* BL21(DE3) and used as inclusion bodies denatured extracts as described previously (5).

Transcription, Translation, and Translocation Assays—All plasmids were enzymatically linearized (pcDNA4.1-HaPrP plasmids with Apal and pcDNA3.1-HuPrP constructs with SacII) and then transcribed with the T7 CapScribe kit (Promega). After integrity verification, the transcribed mRNAs

* This work was supported by Grants SAF2006-00418 (to M. G.) and FIS PI050912 (to M. C.) from the Ministerio de Ciencia e Innovación (to M. G.) and Grant FOOD-CT-2004 506579 (M. G.) from the European Union. The costs of publication of this article were defrayed in part by the payment of page charges. This article must therefore be hereby marked "advertisement" in accordance with 18 U.S.C. Section 1734 solely to indicate this fact.

¹ To whom correspondence should be addressed: Insto Química-Física "Rocasolano," CSIC, Serrano 119, 28006 Madrid, Spain; Tel: 34915619400, Fax: +34915612431, E-mail: mgasset@iqfr.csic.es.

² The abbreviations used are: PrP, prion protein; PrP^C, cellular prion protein; PrP(M15), isoform produced by translation starting at Met-15; PrP(M8), isoform produced by translation starting at Met-8; PIPLC, phosphatidylinositol-specific phospholipase C; PBS, phosphate-buffered saline; YFP, yellow fluorescent protein; SUMO, small ubiquitin-like modifier; WT, wild type; PNGase F, peptide N-glycosidase F; PDI, protein disulfide isomerase; CHO, Chinese hamster ovary; Tricine, N-[2-hydroxy-1,1-bis(hydroxymethyl)ethyl]glycine; Ha, Syrian hamster; Hu, human.

were translated at 80 $\mu\text{g}/\text{ml}$ final concentration using the 50% (v/v) nuclease-treated rabbit reticulocyte lysate system (Promega) and RedivueTM L-[³⁵S]methionine (Amersham Biosciences), as indicated by the manufacturer. For translation-translocation assays, the reaction mixture was enriched in 15% (v/v) canine pancreatic rough microsomal membranes (Ref. 24 and references therein). Isolation of the fraction of sealed microsomes from the reaction mixtures was performed by discontinuous sucrose gradient ultracentrifugation as described previously (24). For protease protection analysis, the total reaction mixtures and their sealed microsomal fractions were incubated for 1 h at 4 °C with 0.1 mg/ml proteinase K (Roche Diagnostics) both in the absence and in the presence of 0.5% Triton X-100. The reaction was stopped with 5 mM phenylmethylsulfonyl fluoride. The ³⁵S-labeled reaction products were immunoprecipitated with αPrP 3F4 monoclonal antibody (Signet Laboratories), resolved on Tris-Tricine 16.5% SDS-PAGE gels, and visualized using a phosphorimaging device (Fuji FLA-3000). Enzymatic deglycosylation was performed by incubating the immunoprecipitated samples with PNGase F (New England Biolabs) according to the manufacturer's instructions.

Cell Culture, Transfections, and Treatments—CHO and COS-7 cells were grown and maintained in Dulbecco's modified Eagle's medium supplemented with 10% fetal bovine serum, 2 mM glutamine, 10 IU/ml penicillin, and 10 $\mu\text{g}/\text{ml}$ streptomycin in a humidified atmosphere of 5% CO₂ at 37 °C. Transfection of cells with the different plasmids was performed with TransIT-LT1 (Mirus) following the manufacturer's instructions. After 48 h, cells were processed for Western blotting. For bulk selection of stable transfectants, cells were subjected to selection experiments, 24 h after transfection. For translocation experiments, 24 h after transfection, the absence or presence of 5 mM proteinase K was tested. Alternatively, after 4 h, the medium was replaced with fresh medium and was continued for another 14 h. Cells were then harvested and analyzed for PrP^C translocation (see below).

Cell Lysates, Brain Homogenates, and Fractionations—Denatured cell lysates were prepared at about 15 mg/ml protein concentration in 62.5 mM Tris-HCl, pH 6.8, containing 4% SDS (w/v) and 25% glycerol (w/v), boiled for 10 min, and then cleared by centrifugation at 15,000 $\times g$ for 20 min. Hamster brains were obtained from the Animal Facility of the Instituto de Investigaciones Biomédicas "Alberto Sols" Universidad Autónoma de Madrid (UAM)-CSIC. Human cortex control samples were obtained from the Institute of Neuropathology and University of Barcelona/Clinic Hospital brain banks following the guidelines of the local ethics committees. Tissue homogenates at 10% (w/v) were prepared in PBS, pH 7.5, containing 0.25 M sucrose, 1.5 mM sodium orthovanadate, 5 mM EDTA, and the EDTA-free Complete protein inhibitor mixture (Roche Diagnostics), aliquoted, and kept at -80 °C. Fractionation of cell and tissue homogenates into nuclear and post-nuclear fractions was performed using the Pure Prep nuclei isolation kit (Sigma) following the manufacturer's indications. The final step including PIPLC digestion was introduced to ensure the removal of contaminant raft-resident PrP^C.

Protein Aggregation Assays—Analysis of PrP aggregation upon proteasome inhibition was performed with minor modifi-

cations to published methods (13, 15–17). Cells were lysed in cold EZ-lysis buffer and then separated into pellet (nuclear) and supernatant (postnuclear) fractions by a 500 $\times g$ centrifugation for 10 min at 4 °C. The pellets were washed twice with EZ-lysis buffer for isolation of the nuclear fractions. The postnuclear supernatants were supplemented with 0.5% Triton X-100 and 0.5% deoxycholate, dispersed by extensive pipetting, and then centrifuged for 10 min at 13,000 $\times g$ at 4 °C. Proteins in the supernatant were precipitated with cold 15% trichloroacetic acid. All protein pellets were resuspended in 0.1 M Tris-HCl, pH 8.0, 1% SDS, and equal aliquots of each fraction were analyzed by SDS-PAGE and immunoblotting.

Immunoprecipitation and Western Blotting—Samples were lysed in 62.5 mM Tris-HCl, pH 6.8, containing 4% (w/v) SDS, and 25% (w/v) glycerol. After a 10-min spin at 10,000 $\times g$, the supernatants were diluted 1:40 with PBS, pH 7.4, containing 0.1% sodium deoxycholate (Calbiochem), 1% Nonidet P-40 (Sigma-Aldrich), 1.5 mM sodium orthovanadate, and 1 mM phenylmethylsulfonyl fluoride. Samples were incubated for 1 h with protein A/G-Sepharose (Amersham Biosciences). After a 5-min centrifugation at 10,000 $\times g$, the supernatants were incubated with αPrP antibodies at 4 °C, and the resulting immunoprecipitates were captured with protein A/G-Sepharose. Samples were resolved on 12.5% SDS-PAGE gels. Proteins (~50 kDa) were transferred to polyvinylidene difluoride membrane. Membrane-bound proteins were probed with αPrP antibody followed by mouse TrueBlot peroxidase-conjugated $\alpha\text{-mouse IgG}$ (1:1000, Pierce and Warriner), goat $\alpha\text{-mouse}$ horseradish peroxidase-conjugated IgG (1:3000, Sigma), or goat $\alpha\text{-rabbit}$ horseradish peroxidase-conjugated IgG (1:8000, Chemicon) and then developed with chemiluminescent Chemicon reagents. Data acquisition and analysis were carried out using the Bio-Rad ChemiDoc equipment. The following primary antibodies and dilutions were used: αPrP 3F4 (1:5000, Signet Laboratories), αPrP SP (1:1000, provided by D. Harris and raised against PrP N-terminal signal peptide), $\alpha\text{-YFP}$ (1:3000, $\alpha\text{-green}$ fluorescent protein AbCam), $\alpha\text{-PDI}$ (1:1000, AbCam), $\alpha\text{-}\beta\text{-coat protein}$ (1:1000, AbCam), $\alpha\text{-histone H3}$ (1:2000, AbCam), $\alpha\text{-ubiquitin P4D1}$ (1:200, Santa Cruz Biotechnology), $\alpha\text{-SUMO-1 D-11}$ (1:200, Santa Cruz Biotechnology), and $\beta\text{-actin}$ (1:5000, Sigma-Aldrich).

Confocal Fluorescence Microscopy—Cells were plated onto glass coverslips, allowed to attach for 24 h, and then transfected for 48 h. Cells were fixed with 4% paraformaldehyde in PBS containing 5% sucrose for 10 min at room temperature and washed three times with PBS. Cells were permeabilized and blocked in PBS containing 0.5% saponin, 0.1% Triton, and 2% bovine serum albumin for 10 min at room temperature. Cells were incubated with αPrP 3F4 (1:600) and with $\alpha\text{-PDI}$ (1:600) for 1 h at room temperature. After three washes with blocking buffer, samples were incubated with Alexa Fluor-647-conjugated goat $\alpha\text{-mouse IgG}$ (1:800), Alexa Fluor-488-conjugated $\alpha\text{-rabbit IgG}$ (1:800), and Hoechst 33342 (10 $\mu\text{g}/\text{ml}$) in blocking solution for 30 min at room temperature. After washing, the coverslips were mounted on glass slides with ProLong Gold antifade reagent (Molecular Probes). Images were captured with a confocal microscope (Leica TCS-SP-AOBS-UV) using

WITHDRAWN
October 27, 2017

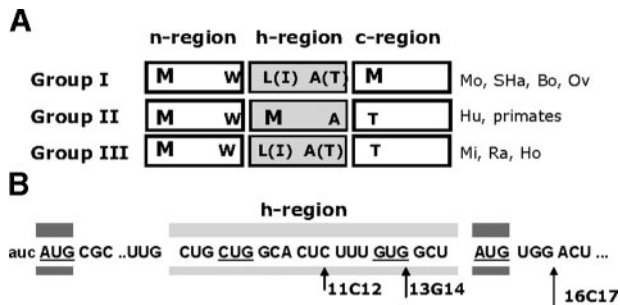


FIGURE 1. Alternative translation start sites in the PrP mRNA signal sequence coding region. A, classification of PrP signal sequence based on the presence of Met residues at the h-region boundaries. Mo, mouse; Bo, bovine; Ov, ovine; Mi, mink; Ra, rabbit; Ho, horse. B, potential translation start sites in the HaPrP signal sequence mRNA coding region. AUG (thick) and non-AUG (thin) triplets are underlined. Arrows indicate the positions of insertions used for reading frame shifts in the generation of the 11C12, 13G14, and 16C17 mutants. M, W, T, L, and I correspond to amino acid residues using the one-letter code.

the UV and argon lasers at 20 milliwatt for excitations at 364 nm (Hoescht) and 488 nm (Alexa Fluor-488), respectively, and the 633-nm line of the He-Ne laser at 10 milliwatt for excitation at 647 nm. Image analysis was performed using Leica confocal software.

Cell Proliferation Assays and Cell Cycle Analysis—For cell growth analysis, cells were co-transfected with pEYFP (Clontech) and the plasmid coding wild type HaPrP or its mutants. After 48 h of transfection, cells were synchronized in G1 by serum deprivation for 18 h and then released by replating in fresh medium for 6 h. Cell proliferation was analyzed in triplicate using the bromodeoxyuridine (BrdU) incorporation assay (Roche) and a MR500 microplate reader (Biochem) and a MR500 microplate reader (Biochem). BrdU incorporation was determined by flow cytometry using a FACSCalibur flow cytometer (BD Biosciences). In this experiment, cells were selected by cell sorting before BrdU incorporation. Data were compared by one- or two-way analysis of variance with Bonferroni's post-test analysis using GraphPad Prism v 4.0.

RESULTS

N-terminal Signal Peptides of PrP Contain a Dual Methionine Motif—N-terminal signal peptides display a tripartite organization into n-, h-, and c-regions, with the hydrophobic central region (h-region) essential for co-translation membrane integration and translocation process. The signal sequences of PrP from different species can be classified into three groups on the basis of the number of Met residues and their position with respect to regional boundaries (Fig. 1). Group I, represented by the rodent sequences, contains two Met residues at positions 1 and 15; the second position is in the N-terminal side of the c-region. In Group II, represented by the human sequence, the two Met residues are at positions 1 and 8. In this case, the second Met constitutes the N terminus of the h-region. On the contrary, Group III, which is represented by the mink sequence, lacks the second Met residue. When converted into their cognate mRNA sequences, the Met residues of the signal sequences become AUG codons that could behave as

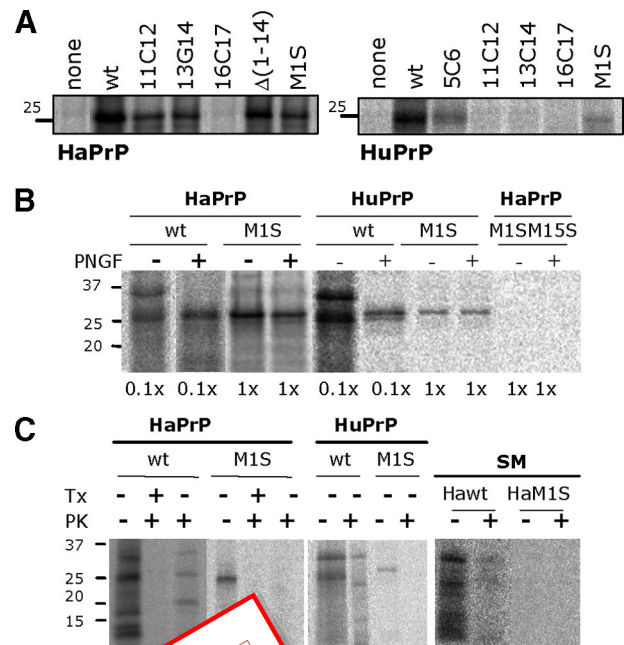


FIGURE 2. Translation of PrP mRNA. A, *in vitro* translation of the mRNA of HaPrP (wt, M1S) and of their signal sequence mutants. B, cell-free translation of HaPrP (wt, M1S), HuPrP (wt, M1S), and HaPrP (M1S/M1S) mutants in the presence of pancreatic microsomes and then immunoprecipitated with anti-PrP antibody. The immunoprecipitates were analyzed by SDS-PAGE. Relative sample loads are indicated at the bottom. C, cell-free translation of HaPrP (wt, M1S) and HuPrP (wt, M1S) mutants in the presence of pancreatic microsomes and then immunoprecipitated with anti-PrP antibody. The immunoprecipitates were analyzed by SDS-PAGE. Relative sample loads are indicated at the bottom. D, cell-free translation of HaPrP (wt, M1S) and HuPrP (wt, M1S) mutants in the presence of pancreatic microsomes and then immunoprecipitated with anti-PrP antibody. The immunoprecipitates were analyzed by SDS-PAGE. Relative sample loads are indicated at the bottom.

translation initiation sites. We also identified two in-frame triplets (CUG and GUG coding HaPrP L9 and V13) that could sustain translation initiation by means of a single base difference. These non-AUG codons are conserved in all species. If used, any of these codons could yield nascent chains with different cellular fates.

The MM Motif Allows a Dual Translation Start and the Existence of PrP Isoforms—To test whether the downstream AUG codons found in the signal sequence regions of PrP mRNA in Group I and Group II could sustain translation initiation, we generated a series of point mutations in both the HaPrP and the HuPrP open reading frames (Figs. 1 and 2 and Table 1). These mutations consisted of the insertion of a C or a G at various positions causing a +1 shift in the reading frame (11C12, 13G14, 16C17), as well as an Met-to-Ser substitution (ATG-to-TTC). The reading frameshift mutations allow the study of both non-AUG and AUG start sites, whereas the Met-to-Ser substitutions permit the evaluation of the role of a specific Met residue. It should be noted that frameshift mutations allow translation initiation at either start site, but only the product produced from the start site downstream from the insertion will proceed to the wild type (WT) stop codon and will produce chains retaining the 3F4 PrP epitope.

TABLE 1**HaPrP and HuPrP constructs**

The HaPrP open reading frame, cloned into pcDNA4.1 under BglII/EcoRI targets, and the HuPrP open reading frame, cloned into pcDNA3.1 under BamHI/EcoRI targets, were used as templates for the generation of point, reading shift, and deletion mutants using standard molecular biology protocols.

Name	Mutation	Forward oligonucleotide
HaPrPwt		
HaPrP(M1S)	ATG-1-TTC	5'-GATCTACCTTCGCGAACCTTAGC-3'
HaPrP(M15S)	ATG-15-TTC	5'-CTCTTTGTGGCTTTCTGGACTGATGTTGG-3'
HaPrP(M1S,M15S)	ATG-1-TTC ATG-15-TTC	5'-CTCTTTGTGGCTTTCTGGACTGATGTTGG-3'
HaPrP(11C12)	+1 shift downstream codon 11	5'-CTCTTTGTGGCTTTCTGGACTGATGTTGG-3'
HaPrP(13G14)	+1 shift downstream codon 13	5'-CTCTTTGTGGCTTTCTGGACTGATGTTGG-3'
HaPrP(16C17)	+1 shift downstream codon 16	5'-GTGGCTATGTGGCTGATGTTGGC-3'
HaPrP(Δ 14)	Deletion of the 1–14 region	5'-CTGCTGGCACTCAGATCTATGTGGACTGAT-3'
HuPrP WT		
HuPrP(M1S)	ATG-1-TTC	5'-GGTACCGAGTTCGGATCCGTCATTTTG-3'
HuPrP(M8S)	ATG-8-TTC	5'-CTGGCTGCTGGTTCTGGTTCTCTTTG-3'
HuPrP(M1S,M8S)	ATG-1-TTC ATG-8-TTC	5'-GGTACCGAGTTCGGATCCGTCATTTTG-3'
HuPrP(5C6)	+1 shift downstream codon 5	5'-CTGGCTGCTGGTTCTGGTTCTCTTTG-3'
HuPrP(11C12)	+1 shift downstream codon 11	5'-GCGAACCTTGGCCTGCTGGATGCTGG-3'
HuPrP(13C14)	+1 shift downstream codon 13	5'-GCTGGATGCTGGTTCTCTTTTGGCCACATGG-3'
HuPrP(16C17)	+1 shift downstream codon 16	5'-CTGGTTCTCTTTGTGGCCACATG-3'
		5'-GTGGCCACATGGCAGTACCTGGGC-3'

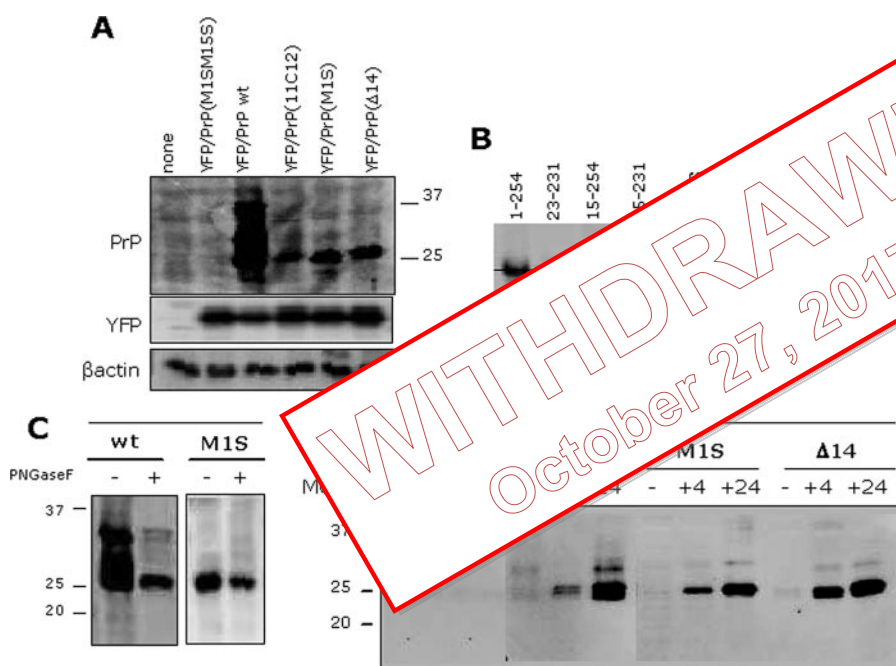


FIGURE 3. Expression of HaPrP(M15) in CHO cells. A, transient expression of HaPrP WT and of its mutants in CHO cells. After 48 h of co-transfection with pEYFP, cells were harvested, lysed, and immunoblotted with antibodies against PrP (3F4), YFP, and β -actin, respectively. Similar results were obtained using COS-7 cells. B, comparison of HaPrP(M15) with 1–254, 15–254, 15–231, and 23–231 PrP chains produced in *E. coli* inclusion bodies by Western blot. The Tris-Tricine SDS-PAGE was performed using 16.5% gels, and the blot was probed with 3F4. The migration of the recombinant PrP-(15–254) chain is depicted with a straight line. C, enzymatic deglycosylation with PNGase F of HaPrP WT and of its M15 mutant. D, incorporation of HaPrP WT and of its M15 and Δ 14 mutants into cytosolic insoluble aggregates upon proteasome inhibition. After transfection (30 h), cells were treated in the absence or presence of 5 μ M MG132. Incubation with MG132 was allowed to proceed for either 24 h (+24) (irreversible inhibition) or after 4 h (+4), the medium were replaced with MG132-free medium, and the incubation was continued for other 16 h (transient inhibition). Insoluble cytosolic aggregates were isolated as described under “Experimental Procedures.”

The results of the translation of the mRNAs coding for WT and mutant HaPrP and HuPrP using reticulocyte lysates followed by immunoprecipitation with 3F4 are shown in Fig. 2A. In agreement with previous reports, wild type HaPrP mRNA was translated into a major polypeptide chain of about 26 kDa. Under the same conditions, translation of the mRNA coding HaPrP(M1S), in which the canonical AUG is functionally impaired, and for the reading frameshift mutants

HaPrP(11C12) and HaPrP(13G14) led to the production of a single product of similar mass (26 kDa) but with reduced intensity (about 5% of that of the WT). On the contrary, translation of the mRNAs HaPrP(16C17) and HaPrP(M1S,M15S) resulted in the absence of any detectable signal. These results support the idea that HaPrP mRNA contains a minor translation initiation site and that this site is located at codon 15, the AUG triplet coding for Met-15. It should be noted that the chains translated from Met-1 and Met-15 could not be easily differentiated by electrophoresis, probably as a result of the balance between the differences in size and hydrophobicity of the chains (25).

The translation of WT HuPrP mRNA yielded a band corresponding to a polypeptide chain of about 27 kDa (Fig. 2A). This band was detected using the mRNAs of the HuPrP(M1S) and HuPrP(5C6) mutants but with less intensity. On the contrary, this band was not observed using the mRNAs of the HuPrP(11C12), HuPrP(13C14), HuPrP(16C17), and HuPrP(M1S,M8S) mutants. These results show that HuPrP mRNA, as model for Group II, also contains a minor translation start site and that this site is located at codon 8, the AUG triplet coding for Met-8. Because the alternative translation start site of PrP signal sequences in groups I and II is due to the dual methionine motif, it follows that the sequences of Group III either lack this capacity or utilize a different process.

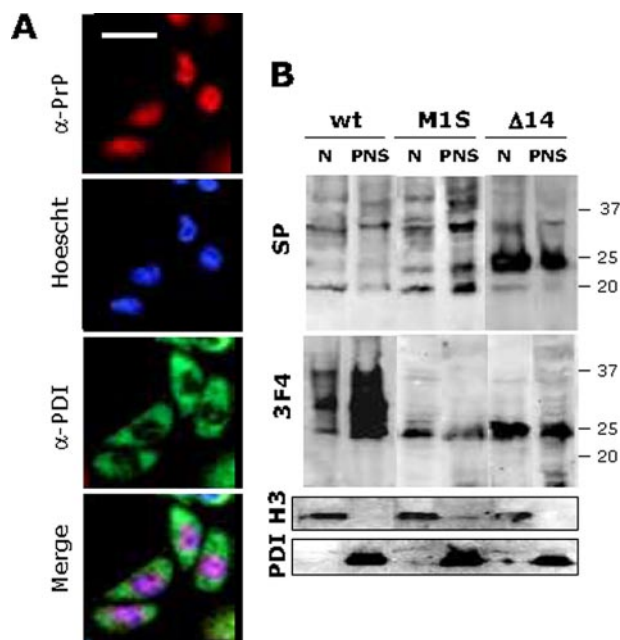


FIGURE 4. Subcellular location of HaPrP(M15) in CHO cells. *A*, indirect immunofluorescence of CHO cells transiently transfected with HaPrP(Δ 14). Fixed and permeabilized cells were stained with antibodies against PrP (3F4, red) and PDI (endoplasmic reticulum marker, green), and with the nuclear dye Hoechst (blue). The white bar represents 40 μ m. *B*, partitioning of PrP between the nuclear (N) and the postnuclear (PNS) fractions of transiently transfected CHO cells with HaPrP WT and its mutants. The displayed immunoblots were probed with α -PrP (3F4 and α -SP), α -histone H3 (nuclear marker, around 30 kDa), and α -PDI (endoplasmic reticulum marker, around 60 kDa).

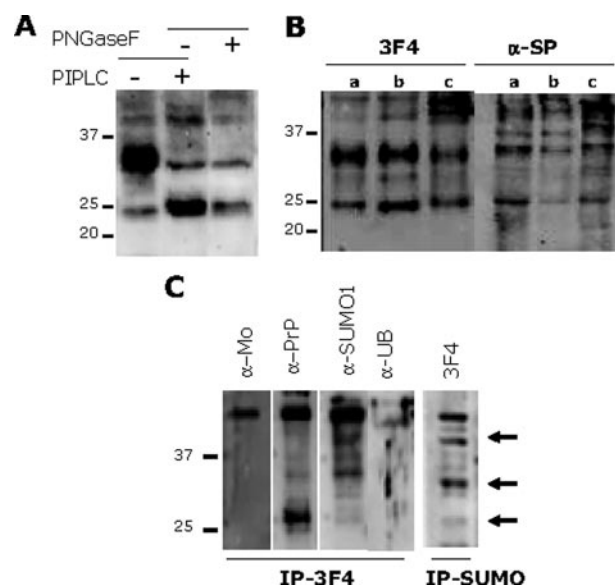


FIGURE 5. Analysis of the nuclear PrP isoform in normal brain homogenates. *A*, removal of raft-associated PrP species from purified nuclei. Nuclei purified from hamster brain homogenates were digested with PIPLC and then centrifuged to remove phosphatidylinositol-bound co-purifying proteins. PIPLC was digested in the absence and presence of PNGase F. *B*, PrP forms in PIPLC-treated nuclei from hamster brain homogenates, immunoprobed with 3F4 and α -SP. *C*, nuclear fractions purified from control and 3F4 α -PrP-containing nuclei were immunoprobed with antibodies: mouse TrueBlot (α -Mo), 3F4 α -PrP, α -SUMO1, α -UB, and 3F4 α -PrP.

HaPrP(M15) and HuPrP(M8) Isoforms

Synthesized C^{yt} PrP—To unambiguously establish the relationship between HaPrP(M15) and HuPrP(M8) and the synthesized C^{yt} PrP, we studied their localization and glycosylation states (Fig. 2, *B* and *C*). Fig. 2*B* shows that the mRNAs, the products of mRNAs, and the translated proteins of microsome membranes consisted of a single band of ~26 kDa that remained unchanged after PNGase F digestion. Comparison of the bands after deglycosylation, in particular of HuPrP chains, suggests that HuPrP(M15) migrates similarly to an unprocessed full-length chain (see below) (26). The unglycosylated pattern agrees with a cytosolic location for the HaPrP(M15) and HuPrP(M8) C-terminal domains. Furthermore, external addition of proteinase K to both the total reaction mixture and its sealed microsome fraction (no signal was detected in this fraction even using a 10 \times overload as compared with the WT) resulted in complete degradation of the ~26-kDa chains translated from the HaPrP(M15) and HuPrP(M8) mRNAs (Fig. 2*C*). In contrast, the product translated from WT mRNAs under similar conditions showed protected fragments corresponding to translocated and integrated PrP chains (3). Taken together, these results suggest that HaPrP(M15) and HuPrP(M8) chains segregate outside the secretory route under a proteinase K-sensitive conformation as described for C^{yt} PrP.

To determine whether the synthesis of these isoforms takes place in cellular contexts, we proceeded with transient transfection experiments using CHO and COS-7 cells, which have undetectable levels of endogenous PrP expression. In this case, the study was restricted to the HaPrP sequences for biosafety

was performed as co-transfection with pEYFP to monitor PrP expression as an internal control. Plasmids encoding HaPrP WT and HaPrP(M15M15S) were used as positive and negative controls for PrP C expression, respectively, whereas those encoding HaPrP(11C12) and HaPrP(M1S) were employed to assess the functionality of M15 as start site. Fig. 3*A* shows that HaPrP(M15) was indeed synthesized by cells based on the presence of a 26-kDa band recognized by α -PrP 3F4 in the lysates of HaPrP(11C12) and HaPrP(M1S) transfectants. Importantly, the 26-kDa band was also recognized by α -SP, an antibody raised against the C-terminal region of the signal sequence (11). In cell lysates, HaPrP(M15) retained the C-terminal hydrophobic segment according to electrophoretic mobility determinations using a panel of recombinant PrP chains consisting of the full unprocessed chain (1–254 sequence), the fully processed chain (23–231 sequence), and N-terminally shortened chains either containing (15–254) or lacking (15–231) the C-terminal hydrophobic segment (Fig. 3*B*).

To corroborate that the HaPrP(M15) synthesized in cells behaves as C^{yt} PrP, we studied its glycosylation state as well as its capacity to form insoluble aggregates upon proteasome impairment (13, 15–17). Fig. 3*C* shows that in contrast to WT HaPrP, 26-kDa HaPrP(M15) remained unchanged upon PNGase F digestion as expected for C^{yt} PrP. Moreover, both transient and irreversible inhibition of the proteasome with 5 μ M MG132 promoted the formation in the cytosol of insoluble HaPrP(M15) aggregates (Fig. 3*D*). Both the absence of glycosylation and the capacity to form cytosolic insoluble aggregates confirms that HaPrP(M15) behaves as C^{yt} PrP in a cellular context.

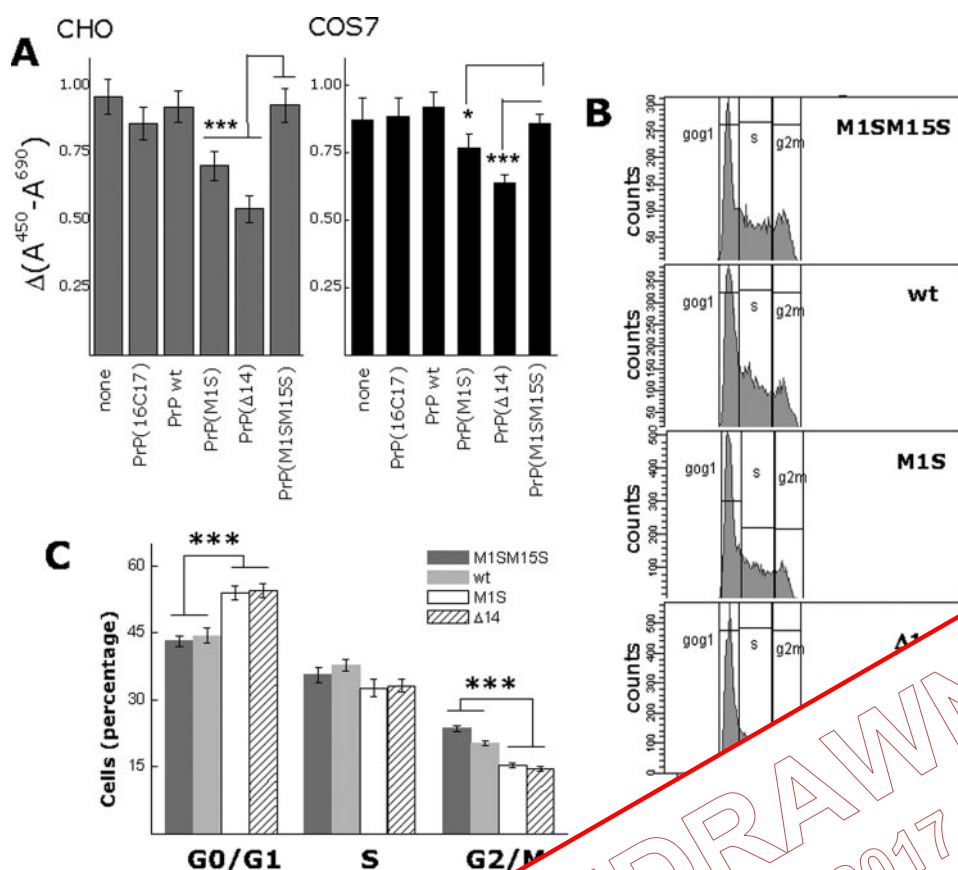


FIGURE 6. HaPrP(M15) expression interferes with cell growth. A, growth of CHO and COS7 cells expressing various PrP constructs. Data are shown as the mean \pm S.D. of three independent experiments. B, typical cell cycle profile of YFP-selected CHO cells expressing various PrP constructs. C, cell cycle phase percentages of YFP-selected CHO cells expressing various PrP constructs. Data are shown as the mean \pm S.D. of three independent experiments. Statistical significance is indicated by asterisks (*, $p < 0.05$; **, $p < 0.01$; ***, $p < 0.001$). For both panels, A and B, the relative expression level of the constructs was similar to that displayed in Fig. 3A.

HaPrP(M15) and HuPrP(M8) Are Found in Nuclei Isolated from Cells and Normal Brain Homogenates and Are Sumoylated—To elucidate the properties of these isoforms, we first studied their subcellular location using confocal microscopy. Unless stated, HaPrP(M15) was expressed from the HaPrP($\Delta 14$) construct for easier detection. Indirect immunofluorescence stainings showed that at 48 h after transfection, HaPrP(M15) was localized largely to the nuclei of cells (Fig. 4A). The distribution pattern agreed with the diffuse nucleoplasmic location observed for several studied C^{yt} PrP models (19, 27) and differed from the intranuclear granules observed in neuronal cells expressing bovine PrP^C (28). The nuclear localization was then confirmed by subcellular fractionation of cell homogenates. Fig. 4B shows that about 70% of the expressed HaPrP($\Delta 14$) was localized to the nuclear fraction, mainly as a 26-kDa chain but also as higher molecular weight species. Similar results were obtained using CHO and COS-7 cells.

To generalize the nuclear localization of HaPrP(M15), as well as to determine the origin of the high molecular weight bands, we purified the nuclei from normal hamster brain and human

cortex homogenates and characterized the PrP contained therein. Before the analysis, the purified nuclei were dispersed in EZ-lysis buffer, digested with PIPLC, and then centrifuged at low speed. This process allows the release of the contaminant membrane-anchored forms (29). Fig. 5A shows that after removing raft-resident PrP^C, PrP was detected in the nuclei purified from hamster brain homogenates as two bands of 26 and 35 kDa that remained unchanged after enzymatic deglycosylation. Nuclear PrP in human cortex was also comprised of two major PNGase F-resistant bands of about 26 and 35 kDa. These bands were recognized by both 3F4 and SP, as expected from PrP chains bearing N-terminal shortened signal peptides (Fig. 5B). These data confirm the existence and nuclear localization of isoforms produced by de novo translation in normal

The complexity of the bands suggests the occurrence of covalent modifications. Of the modifications that can occur in nuclear proteins and cause increases in size, activity-modifying sumoylation and degradation-targeting ubiquitinylation were studied. Fig. 5C shows that high molecular weight bands of PrP immunoprecipitated with 3F4 from denatured nuclei extracts of hamster brain homogenates were recog-

nized by an anti-SUMO-1 antibody but not by anti-ubiquitin or anti-SUMO 2/3 antibodies. Inverse pull-down experiments with α -SUMO-1 confirmed 3F4 immunoreactivity. Because SUMO-1 conjugation involves the covalent attachment of a single 9.5-kDa chain, the observed band pattern can be explained to a large extent by considering the composition of a non-sumoylated chain (26 kDa) and a SUMO-1-conjugated form (35 kDa). In summary, PrP(M8/M15) appear to be a nuclear isoform that acts as substrate for SUMO-1 conjugation.

HaPrP(M15) Expression Abrogates Cell Proliferation—Trials to establish cell lines expressing HaPrP(M15) were unsuccessful despite the absence of a conclusive and reproducible cell death event. Stably transfected clones were selected, but they failed to grow. These growth alterations together with the nuclear distribution and involvement of reversible sumoylation prompted us to consider a possible antiproliferative activity.

Analysis of bromodeoxyuridine incorporation showed that HaPrP(M15) did indeed decrease cell growth as compared with HaPrP WT and the negative control HaPrP(M1SM15S) in both COS-7 and CHO cells (Fig. 6A). This effect was more pro-

nounced and statistically significantly higher ($p < 0.001$) for the HaPrP($\Delta 14$) mutant, which overexpresses the PrP isoform (Fig. 3A), than for the HaPrP(M15) and HaPrP(11C12) mutants.

The cell cycle was then analyzed using a co-transfection approach. In this case, cells were co-transfected with pEYFP for separation of the positive transfectants by cell sorting before propidium iodide labeling. Fig. 6, B and C, shows that cells expressing HaPrP(M15) from both HaPrP($\Delta 14$) and HaPrP(11C12) constructs exhibited a higher proportion of cells in the G_0/G_1 phase as compared with the mock control (transfection with HaPrP(M15M15S)). These results indicate that HaPrP(M15) functions as a growth suppressor that delays the exit from G_1 phase.

DISCUSSION

In this study, we have shown that the minor member of the PrP^C family segregating outside the secretory route is generated by alternative initiation of translation. The presence of a second Met residue at the h-region boundary of the signal sequence determines the alternative translation initiation event. This process permits the synthesis of an isoform translated either from Met-15 in HaPrP or from Met-8 in HuPrP. This isoform represents a novel chain differing from the conventional mature form in the retention of the c-region of the N-terminal signal sequence and the full C-terminal hydrophobic region. These two segments could provide new functions as structural regulators or as sites of interaction for distinct ligands and others.

The use of in-frame alternative translation is a relatively common process by which a single mRNA can acquire a multiple protein products under environmental regulation. The proportion of PrP(M15) synthesis was studied *in vitro* studies and in the cell system. PrP(M15) might be susceptible to such modulation supported by the cell and regional dependence of PrP synthesis in normal rodent brains as well as its increased levels in the endoplasmic reticulum stress (23, 35). As noted, the dual start site motif is missing in a group of highly conserved PrP sequences. In these sequences, the AUG triplet coding for Met-15 is found as either ACG or ACA, which code for Thr. Of these two codons, ACG can function as a non-AUG start site (36, 37). However, the function of the ACA triplet as a start is unclear; thus whether ACA-bearing species use the alternative translation mechanism remains to be established.

Isolating the synthesis of HaPrP(M15) from that of the major membrane-bound PrP forms allowed three major findings: nuclear localization, variable SUMO-1 conjugation, and antiproliferative activity. The nuclear localization of this isoform might explain results of previous PrP studies describing rare nuclear localization, the presence of nuclear localization sequence, and the capacity of the chain to interact with nucleic acids and with chromatin (19, 28, 38).

SUMO-1 conjugation of the nuclear population of PrP suggests stringent regulation of activity and physiological relevance for this isoform. In general, sumoylation provides an on/off functional switch for protein interactions involved in processes such as transport, transcriptional silencing, genomic

stabilization, and stress responses (39). SUMO-1-conjugated and free HaPrP(M15) chains might thus represent alternative functional states of the molecule. It is thus interesting to note that the degree of sumoylation in nuclei from brains was higher than that in cells. With the limitations imposed by the lack of sumoylation control, HaPrP(M15) expression might be involved in dysregulation of cellular growth resulting in G_0/G_1 phase arrest.

The antiproliferative function of HaPrP(M15) expands the physiological role of PrP^C. Because most cells withdraw from the cell cycle to differentiate during the G_1 phase, it is tempting to consider HaPrP(M15) as candidate for promotion of G_1 phase arrest required for cell differentiation in some developing tissues (7). On the other hand, the loss of HaPrP(M15) nuclear functionality might favor either cell transformation on depletion (8) or cell death on cytosolic accumulation (15). HaPrP(M15) can regulate the efficiency of prion accumulation, which decreases with cell division (40). The isolation of the synthesis of this isoform from that of other members of the PrP^C family suggests that each member of this family might have different physiological roles and that their aberrant cross-talk could play a pathogenic mechanism.

We thank Dr. M. Seisdedos for technical assistance, Dr. S. Hegde, C. Korth, J. Fomina, and Dr. M. Seisdedos for sharing reagents and for

1. Prusiner, S. B., and Polymenidou, M. (2004) *Cell* **116**, 313–327
2. Gasset, M., Baldwin, M. A., Lloyd, D. H., Gabriel, J. M., Holtzman, D. M., Cohen, F., Fletterick, R., and Prusiner, S. B. (1992) *Proc. Natl. Acad. Sci. U. S. A.* **89**, 10940–10944
3. Hegde, R. S., Mastrianni, J. A., Scott, M. R., DeFea, K. A., Tremblay, P., Torchia, M., DeArmond, S. J., Prusiner, S. B., and Lingappa, V. R. (1998) *Science* **279**, 827–834
4. Chiesa, R., and Harris, D. A. (2001) *Neurobiol. Dis.* **8**, 743–763
5. González-Iglesias, R., Pajares, M. A., Ocal, C., Espinosa, J. C., Oesch, B., and Gasset, M. (2002) *J. Mol. Biol.* **319**, 527–540
6. Caughey, B., and Baron, G. S. (2006) *Nature* **443**, 803–810
7. Steele, A. D., Emsley, J. G., Ozdinler, P. H., Lindquist, S., and Macklis, J. D. (2006) *Proc. Natl. Acad. Sci. U. S. A.* **103**, 3416–3421
8. Liang, J., Pan, Y., Zhang, D., Guo, C., Shi, Y., Wang, J., Chen, Y., Wang, X., Liu, J., Guo, X., Chen, Z., Qiao, T., and Fan, D. (2007) *FASEB J.* **21**, 2247–2256
9. Hölscher, C., Bach, U. C., and Dobberstein, B. (2001) *J. Biol. Chem.* **276**, 13388–13394
10. Kim, S. J., Rahbar, R., and Hegde, R. S. (2001) *J. Biol. Chem.* **276**, 26132–26140
11. Stewart, R. S., and Harris, D. A. (2003) *J. Biol. Chem.* **278**, 45960–45968
12. Hegde, R. S., and Rane, N. S. (2003) *Trends Neurosci.* **26**, 337–339
13. Ma, J., and Lindquist, S. (2002) *Science* **298**, 1785–1788
14. Ma, J., Wollmann, R., and Lindquist, S. (2002) *Science* **298**, 1781–1785
15. Rane, N. S., Yonkovich, J. L., and Hegde, R. S. (2004) *EMBO J.* **23**, 4550–4559
16. Ma, J., and Lindquist, S. (2001) *Proc. Natl. Acad. Sci. U. S. A.* **98**, 14955–14960
17. Yedidia, Y., Horonchik, L., Tzaban, S., Yanai, A., and Taraboulos, A. (2001) *EMBO J.* **20**, 5383–5391
18. Drisaldi, B., Stewart, R. S., Adles, C., Stewart, L. R., Quaglio, E., Biasini, E., Fioriti, L., Chiesa, R., and Harris, D. A. (2003) *J. Biol. Chem.* **278**, 21732–21743

19. Crozet, C. J., Vezilier, J. V., Delfieu, V., Nishimura, T., Onodera, T., Casanova, D., Lehmann, S., and Beranger, F. (2006) *Mol. Cell Neurosci.* **32**, 315–323
20. Rambold, A. S., Miesbauer, M., Rapaport, D., Bartke, T., Baier, M., Win-klhofer, K. F., and Tatzelt, J. (2006) *Mol. Biol. Cell* **17**, 3356–3368
21. Wang, X., Wang, F., Arterburn, L., Wollmann, R., and Ma, J. (2006) *J. Biol. Chem.* **281**, 13559–13565
22. Roucou, X., Guo, Q., Zhang, Y., Goodyer, C. G., and LeBlanc, A. C. (2003) *J. Biol. Chem.* **278**, 40877–40881
23. Orsi, A., Fioriti, L., Chiesa, R., and Sitia, R. (2006) *J. Biol. Chem.* **281**, 30431–30438
24. Hegde, R. S., and Lingappa, V. R. (1996) *Cell* **85**, 217–228
25. Schägger, H. (2006) *Nat. Protoc.* **1**, 16–22
26. Ott, C. M., and Lingappa, V. R. (2004) *Biochemistry* **43**, 11973–11982
27. Lorenz, H., Windl, O., and Kretzschmar, H. A. (2002) *J. Biol. Chem.* **277**, 8508–8516
28. Hosokawa, T., Tsuchiya, K., Sato, I., Takeyama, N., Ueda, S., Tagawa, Y., Kimura, K. M., Nakamura, I., Wu, G., Sakudo, A., Casalone, C., Mazza, M., Caramelli, M., Takahashi, H., Sata, T., Sugiura, K., Baj, A., Toniolo, A., and Onodera, T. (2008) *Biochem. Biophys. Res. Commun.* **366**, 657–663
29. Say, I. H., and Hooper, N. M. (2007) *Proteomics* **7**, 1059–1564
30. Levine, C. G., Mitra, D., Sharma, A., Smith, C. L., and Hegde, R. S. (2005) *Mol. Biol. Cell* **16**, 279–291
31. Touriol, C., Bornes, S., Bonnal, S., Audigier, S., Prats, H., Prats, A. C., and Vagner, S. (2003) *Biol. Cell* **95**, 169–178
32. Sasaki, A., Inagaki-Ohara, K., Yoshida, T., Yamanaka, A., Sasaki, M., Yasukawa, H., AKoromilas, A. E., and Yoshimura, A. (2003) *J. Biol. Chem.* **278**, 2432–2446
33. Sorensen, V., Nilsen, T., and Wiedlocha, A. (2006) *BioEssays* **28**, 504–514
34. Rogers, G. W., Jr., Edelman, G. M., and Mauro, V. P. (2004) *Proc. Natl. Acad. Sci. U. S. A.* **101**, 2794–2799
35. Mironov, A., Jr., Latawiec, D., Wille, H., Bouzamondo-Bernstein, E., Legname, G., Williamson, R. A., Burton, D., DeArmond, S. J., Prusiner, S. B., and Peters, P. (2003) *J. Neurosci.* **23**, 7183–7193
36. Mehdi, H., Ono, E., and Gupta, K. C. (1990) *Gene (Amst.)* **91**, 173–178
37. Chang, K. J., Lin, G., Men, L. C., and Wang, C. C. (2006) *J. Biol. Chem.* **281**, 7775–7783
38. Derrington, E., Gabus, C., Leblanc, P., Chnaidermann, J., Grave, L., Dormont, D., Swietnicki, W., Morillas, M., Marck, D., Nandi, P., and Darlix, J. L. (2002) *C. R. Biol.* **325**, 17–23
39. Geiss-Friedlander, R., and Melchior, F. (2007) *Nat. Rev. Mol. Cell Biol.* **8**, 947–956
40. Ghaemmaghami, S., Phuan, P. W., Perkins, B., Ullman, J., May, B. C., Cohen, F. E., and Prusiner, S. B. (2007) *Proc. Natl. Acad. Sci. U. S. A.* **104**, 17971–17976

WITHDRAWN

October 27, 2017

Biosynthesis of Prion Protein Nucleocytoplasmic Isoforms by Alternative Initiation of Translation

María E. Juanes, Gema Elvira, Aranzazu García-Grande, Miguel Calero and María Gasset

J. Biol. Chem. 2009, 284:2787-2794.

doi: 10.1074/jbc.M804051200 originally published online December 5, 2008

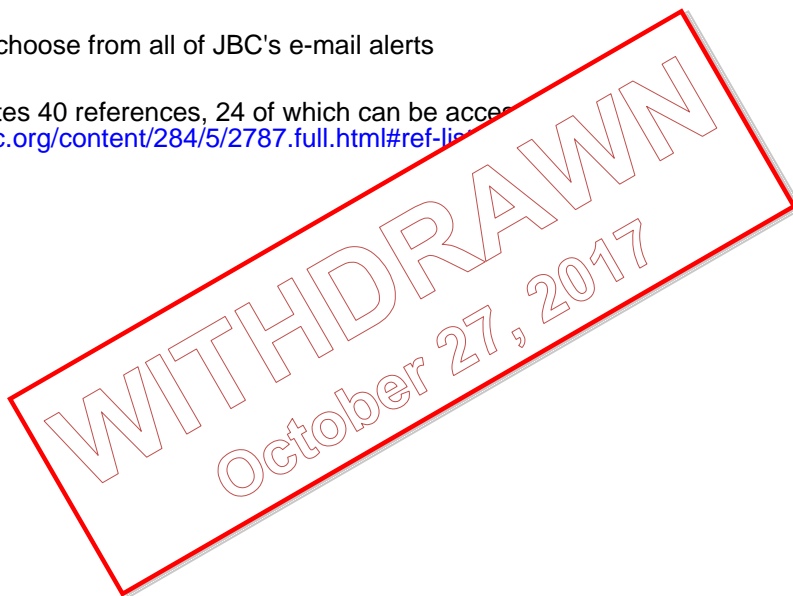
Access the most updated version of this article at doi: [10.1074/jbc.M804051200](https://doi.org/10.1074/jbc.M804051200)

Alerts:

- [When this article is cited](#)
- [When a correction for this article is posted](#)

[Click here](#) to choose from all of JBC's e-mail alerts

This article cites 40 references, 24 of which can be accessed at <http://www.jbc.org/content/284/5/2787.full.html#ref-list-1>



Biosynthesis of Prion Protein Nucleocytoplasmic Isoforms by Alternative Initiation of Translation

María E. Juanes, Gema Elvira, Aranzazu García-Grande, Miguel Calero and María Gasset

J. Biol. Chem. 2009, 284:2787-2794.

doi: 10.1074/jbc.M804051200 originally published online December 5, 2008

Access the most updated version of this article at doi: [10.1074/jbc.M804051200](https://doi.org/10.1074/jbc.M804051200)

Alerts:

- [When this article is cited](#)
- [When a correction for this article is posted](#)

[Click here](#) to choose from all of JBC's e-mail alerts

This article cites 40 references, 23 of which can be accessed free at <http://www.jbc.org/content/284/5/2787.full.html#ref-list-1>

VOLUME 284 (2009) PAGES 2787–2794

DOI 10.1074/jbc.W117.000658

Biosynthesis of prion protein nucleocytoplasmic isoforms by alternative initiation of translation.

María E. Juanes, Gema Elvira, Aranzazu García-Grande, Miguel Calero, and María Gasset

This article has been withdrawn by the authors. We have become aware of errors in the preparation of Figs. 2 and 3, where some lanes appear duplicated. Although replicated experiments performed at the time support the results and conclusions presented in the published paper, we believe that the responsible course of action is to withdraw the article in the interests of maintaining the publication standards of the journal. We apologize for any inconvenience we may have caused. The paper with the corrected figures can be obtained by contacting the authors.